ELSEVIER

Journal of Organometallic Chemistry 569 (1998) 169–175

Journal of Organometallic Chemistry

The reaction of titanocene bis(ferrocenylacetylide) and bis(ruthenocenylacetylide) with silver cation: formation of bis(Ti-tweezers) silver complexes[1]

Yukiko Hayashi [a], Masahisa Osawa [a], Kimiko Kobayashi [a], Takuma Sato [a], Masaru Sato [b], Yasuo Wakatsuki [a,*]

[a] *The Institute of Physical and Chemical Research (RIKEN), Wako, Saitama 351-0198, Japan*
[b] *Chemical Analysis Center, Saitama University, Urawa, Saitama 338-8570, Japan*

Received 4 April 1998

Abstract

Titanocene bis(acetylide) where the acetylide has ferrocenyl or ruthenocenyl terminal group $(C_5H_4R)_2Ti\{(C{\equiv}C)_n\text{-}Mc\}_2$, reacted with 0.5 equivalent amount of $AgPF_6$ giving cationic heptanuclear complexes of the form $[(C_5H_4R)_4Ti_2\{(C{\equiv}C)_n\text{-}Mc\}_4Ag](PF_6)$ (**1a**: R = $SiMe_3$, $n = 1$, Mc = ferrocenyl, **2a**: R = H, $n = 2$, Mc = ferrocenyl, **3a**: R = $SiMe_3$, $n = 2$, Mc = ferrocenyl, **4a**: R = $SiMe_3$, $n = 1$, Mc = ruthenocenyl) in good yields. Likewise, complex $[(C_5H_4SiMe_3)_4Ti_2(C{\equiv}CPh)_4Ag](PF_6)$ (**5a**) was isolated. The Ti(IV)–Fe(II)–Ag(I) complex **3a** was structurally characterized to confirm the solid-state geometry of the first bis(Ti-tweezers) type chelate complex with silver cation in which the silver was coordinated by four triple bonds of the two titanocene bis(acetylide) moieties. The similar Ti(IV)–Ru(II)–Ag(I) complex **4a** was also characterized by single-crystal X-ray analysis. Complex **3a** reacted with 1.5 equivalents (with respect to Ti) of $AgPF_6$ to liberate Fc–$(C{\equiv}C)_4$-Fc (Fc = ferrocenyl) quantitatively.

Keywords: Titanocene bis(acetylide); Ferrocenyl; Ti-tweezers

1. Introduction

We reported recently the synthesis of titanocene bis(-ferrocenylacetylide) and bis(ruthenocenylacetylide) complexes [1,2]. The former complex showed unique redox reactivity, i.e. on oxidation of the two terminal ferrocenyl units by either electrochemical method or silver salt, homolytic splitting of the Ti–C bonds and subsequent coupling of the two acetylide units take place to give 'carbon rod' with neutral ferrocenyl terminal groups in 90–95% yield (Scheme 1). A quite similar reaction was reported later by Lang et al. [3]. Since addition of excess $AgPF_6$ caused oxidation of the ferrocenyl unit of the product and retarded the yield of the desired neutral bis(ferrocenyl) carbon-rod compound, the silver salt had to be added carefully in small potions. On monitoring the reaction by IR $\nu(C{\equiv}C)$ bands, we noticed that addition of ca. 0.5 equivalents $AgPF_6$ gave a new species which, on further addition of $AgPF_6$, liberates progressively the bis(ferrocenyl) carbon-rod as the final product. This intermediate species turned out to be a bis(Ti-tweezers) type complex, formed by aggregation of two starting titanocene bis(acetylide) molecules on one silver cation as described in detail in the present report.

A number of 1:1 complexes of bis(alkynyl)titanocenes with metal fragments $[(C_5H_4R')_2Ti(C{\equiv}CR)_2]M$, have been reported [4–12]. Most of these complexes (M = Ni(CO), $Pt(PR_3)_2$, $FeCl_2$, Co(CO), CuX, CuR, AuR, AgX) display the structure with an embedded M unit between the 'Ti(IV)-tweezers' indicating ability of the bis(alkynyl)titanocene to stabilize a variety of metal fragments via alkynyl ligand bridge. To the best of our knowledge, however, bis(tweezers) type

* Corresponding author. Fax: +81 48 4624665.

[1] Dedicated to Professor Nakamura on the occasion of his retirement from Osaka University.

0022-328X/98/$19.00
PII S0022-328X(98)00785-2

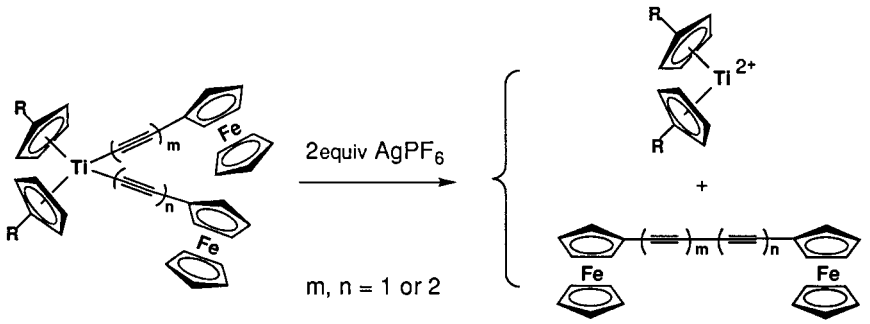

Scheme 1.

2:1 complex of this family has not been reported. There are two precedents though in diphosphineplatinum(II) phenylacetylide chemistry, $[Pt_2(C{\equiv}CPh)_4(dppe)_2Cu]^+$ and $[Pt_2(C{\equiv}CPh)_4(PPh_3)_4Ag]^+$ [13,14]. These platinum complexes are stable, while the Ti(IV)–Fe(II)–Ag(I) counterpart reported here is the prerequisite for the final redox product. Furthermore, some of the complexes reported here have diynyl arms with ferrocenyl end groups: hence their molecular dimension is much larger than those of the reported platinum complexes. Detailed characterization of the new aggregates and its implication for the silver cation-induced coupling of the two acetylide units on Ti have been discussed in the present report.

2. Results and discussion

2.1. Formation of the aggregates

To a CH_2Cl_2 solution of the bis(ferrocenyldiynyl)titanocene complex (**2**), was added $AgPF_6$ in CH_2Cl_2 slowly through a mechanically controlled syringe while the reaction was monitored by IR ν(C≡C) peaks. As the sharp peaks of the starting **2** (2171 and 2021 cm^{-1}) decrease, new peaks grew up at 2161 and 1988 cm^{-1}. At the stage this change was completed, the amount of $AgPF_6$ added was ca. 0.5 equivalents with respect to the moles of **2**. The addition of the solution of $AgPF_6$ was continued which lead to the decrease of 2161 and 1988 peaks with concomitant growth of the peak at 2196 cm^{-1} of the final coupling product, Fc–$(C{\equiv}C)_4$–Fc. When this second change was completed, the total amount of $AgPF_6$ consumed from the beginning was exactly 2 equivalents with respect to starting complex **2**. Apparently the transformation shown in Scheme 1 is a two-stage reaction and the first product appears to be relatively stable.

Isolation of this new product (**2a**) was indeed easily carried out by simply adding 0.5 equivalents $AgPF_6$ to a CH_2Cl_2 solution of **2** and evaporating the solvent after 30 min. It was stable enough to undergo recrystallization. In a similar fashion, three analogs **1a**, **3a** and **4a** were isolated in good yields as crystalline solid (Eq. (1)). The FAB/MS, IR, NMR spectroscopy, and elemental analysis indicated that these were 2:1 adducts of the titanocene bis(acetylide) and $AgPF_6$, of the general form $[(C_5H_4R)_4Ti_2\{(C{\equiv}C)_n\text{-Mc}\}_4Ag](PF_6)$ (Mc = ferrocenyl or ruthenocenyl). These complexes are moderately stable in solution at r.t. but decompose easily by illumination from lamps so that their preparation and purification have to be carried out in dark.

The complexes **1a** and **4a** show the IR ν(C≡C) band at 2015 and 2020 cm^{-1}, respectively, which are ca. 40 cm^{-1} lower energy than those of parent **1** (2056 cm^{-1}) and **4** (2059 cm^{-1}). The diyne complex **2a** exhibits the bands at 2161 and 1988 cm^{-1}, **3a** at 2161 and 1987 cm^{-1} as compared to the corresponding bands of the parent **2** at 2172 and 2021 cm^{-1}, and **3** at 2171 and 2021 cm^{-1}. The lower energy band of the parent complexes, therefore, shifted by ca. 30 cm^{-1} but the shift of the higher energy band was only 10 cm^{-1}. Apparently, silver ion is interacting with one of the triple bonds of the diyne moiety and this was further proved by X-ray structure analysis of **3a** (vide infra.). The structural characterization of the Rc-ethynylene-Ti–Ag aggregate **4a** (Rc = ruthenocenyl) has also been carried out.

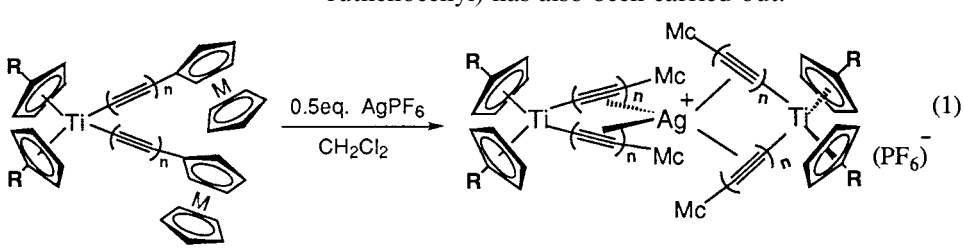

(1)

1 : R=TMS, n=1, M=Fe
2 : R=H, n=2, M=Fe
3 : R=TMS, n=2, M=Fe
4 : R=TMS, n=1, M=Ru

1a : R=TMS, n=1, Mc= ferrocenyl
2a : R=H, n=2, Mc=ferrocenyl
3a : R=TMS, n=2 , Mc=ferrocenyl
4a : R=TMS, n=1, Mc=ruthenocenyl

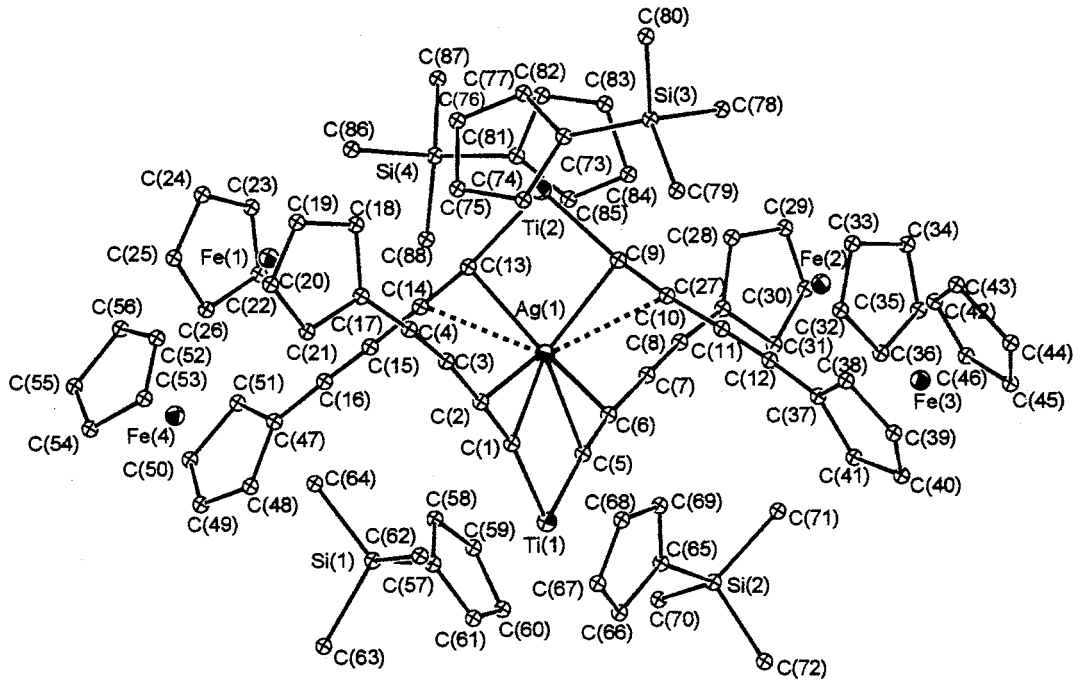

Fig. 1. Molecular structure of the cationic part of **3a** with the atomic numbering scheme.

For comparison, a non-metallocenyl derivative of titanocene acetylide, $(C_5H_4SiMe_3)_2Ti(C{\equiv}C{-}Ph)_2$ (**5**), was treated with $AgPF_6$ (0.5 equimolar relative to Ti) in a similar manner to give again the bis(Ti-tweezers) type complex $[(C_5H_4SiMe_3)_4Ti_2(C{\equiv}C{-}Ph)_4Ag](PF_6)$ (**5a**).

In the Mössbauer spectra of **1a** and **3a** measured at 77 K, only a broad doublet was observed whose IS and QS values were 0.53 and 2.28 mm s^{-1}, respectively. Their Mössbauer parameters are unchanged from those of the parent complexes **1** and **3**; IS = 0.52–0.54 mm s^{-1}, QS = 2.28–2.31 mm s^{-1}, which are typical values for ferrocene derivatives. This indicates that the electronic status of the ferrocenyl group is that of Fe(II) and has not changed before and after the adduct formation with Ag^+.

Although addition of 1.5 equivalents amount of $AgPF_6$ (relative to Ti) to **1a**–**3a** lead to oxidation of the ferrocenyl groups releasing the coupling product Fc–$(C{\equiv}C)_n$–Fc in almost quantitative yields (Scheme 1), a similar reaction of **4a** was not feasible and resulted in decomposition to uncharacterizable precipitate since one-electron oxidation of ruthenocene is difficult [15]. In the case of **5a**, addition of 0.5 equivalents $AgPF_6$ lead to a new species having the $\nu(C{\equiv}C)$ at 2023 cm^{-1}, which we assumed to be a 1:1 complex of **5** and $AgPF_6$. It was not crystalline and on standing its solution or on addition of further $AgPF_6$, it decomposed to intractable material.

All of these observations imply the remarkably high ability of the titanocene bis(acetylide) moiety to chelate a metal unit: even when it has ferrocenyl end group as in **1**–**3**, which is very susceptible to Ag^+, the titanocene bis(acetylide) catches the Ag cation in its tweezers at the initial step of the reaction. Probably because anion PF_6^- is too bulky to have strong direct interaction with Ag^+, the reaction does not form stable 1:1 Ti-tweezers-$AgPF_6$ type complex but proceeds further to form the bis(Ti-tweezers)-Ag^+ aggregate. The Ag^+ trapped in this aggregate, however, can participate in oxidation of the ferrocenyl group at the second stage of the reaction: When more Ag salt is added to the system, some of the four ferrocenyl units of the bis(Ti-tweezers)-Ag^+ aggregate should be oxidized by the second Ag^+ and cause to decrease the electron density at the C≡C triple bonds. Dismissal of the aggregate and re-activation of the initially captured Ag^+ will then follow.

2.2. X-ray structural analysis of *3a* and *4a*

Although crystallization of **3a** in THF afforded good crystals, their size was small. Only metal atoms could be refined with anisotropic thermal parameters because of the limited number of useful peak intensity data. The ORTEP drawing of the cation part is shown in Fig. 1 and the selected structural parameters are listed in Table 1.

The cationic framework has two $(C_5H_4SiMe_3)_2$-$Ti\{(C{\equiv}C)_2{-}Fc)_2$ tweezers units which are oriented almost perpendicularly each other, the dihedral angle Ti(1)–C(1)–C(S)/Ti(2)–C(9)–C(13) being 86(8)°. The Ti(1)–Ag–Ti(2) is linear where Ti–Ag distances are 3.26(1) and 3.19(1) Å in comparison to the Ti–Ag

Table 1
Selected bond lengths (A) and angles (°) for $[(C_5H_4SiMe_3)_4Ti_2(C{\equiv}CC{\equiv}CFc)_4Ag](PF_6)\cdot THF$ (3a·THF)

Ti(1)–C(1)	2.10(4)	Ti(1)–C(5)	2.07(4)
Ti(2)–C(9)	2.12(5)	Ti(2)–C(13)	2.14(4)
Ag–C(1)	2.40(4)	Ag–C(5)	2.38(4)
Ag–C(9)	2.38(5)	Ag–C(13)	2.36(4)
Ag–C(2)	2.68(4)	Ag–C(6)	2.66(5)
Ag–C(10)	2.77(4)	Ag–C(14)	2.81(4)
Ag–Ti(1)	3.26(1)	Ag–Ti(2)	3.19(1)
C(1)–Ti(1)–C(5)	93.9(13)	C(9)–Ti(2)–C(13)	95.8(16)

distance of 3.16(1) Å in a related 1:1 Ti-bis(acetylide)-Ag complex $[(C_5H_4SiMe_3)_2Ti(C{\equiv}C{-}SiMe_3)_2]AgNO_2$ (**6**) [10]. The Ag atom is interacting with four C≡C triple bonds next to the two Ti atoms. Non-equivalent linkages of the Ag atom to C(α) and C(β) carbons of the Ti-acetylide have been reported in **6**, where Ag–C(α) is shorter (2.29(2), 2.33(2) Å) and Ag–C(β) longer (2.41(2), 2.43(2) Å). This tendency is more pronounced in **3a**: Ag–C(α) 2.36(4)–2.40(4) Å; Ag–C(β) 2.66(5)–2.81(4) Å. Particularly the Ag–C(β) bonds are much longer when compared to the corresponding values in **6** apparently owing to the steric reasons.

The Ti–Ru–Ag complex **4a** crystallized in the monoclinic space group C_2/c with one and a half independent molecules. One of the molecules occupy a general position in the unit cell and has crystallographically asymmetric structure while the Ag atom of the other molecule is on the inversion center and therefore this unit has symmetric structure. Since the overall structures of them are almost same, the ORTEP drawing and the selected structural data of the cation part are shown, in Fig. 2 and Table 2, only for the asymmetric molecule.

Table 2
Selected bond lengths (Å) and angles (°) for $[(C_5H_4SiMe_3)_4Ti_2(C{\equiv}CRc)_4Ag](PF_6)$ (4a)

Ti(1)–C(41)	2.13(2)	Ti(1)–C(3)	2.13(2)
Ti(2)–C(5)	2.12(2)	Ti(2)–C(7)	2.11 (1)
Ag–C(1)	2.35(2)	Ag–C(3)	2.40(1)
Ag–C(5)	2.37(1)	Ag–C(7)	2.41(2)
Ag–C(2)	2.81(2)	Ag–C(4)	2.77(1)
Ag–C(6)	2.78(1)	Ag–C(8)	2.72(2)
C(1)–C(2)	1.23(3)	C(3)–C(4)	1.23(3)
C(5)–C(6)	1.24(3)	C(7)–C(8)	1.22(2)
Ag–Ti(1)	3.248(3)	Ag–Ti(2)	3.267(3)
C(1)–Ti(1)–C(3)	93.8(6)	C(5)–Ti(2)–C(7)	93.7(6)
Ti(1)–C(1)–C(2)	165.3(12)	Ti(1)–C(3)–C(4)	172.7(13)
Ti(2)–C(5)–C(6)	162.9(12)	Ti(2)–C(7)–C(8)	170.9(13)

The structural feature of **4a**, whose Ag atom is tetrahedrally coordinated by four acetylene fragments with the dihedral angle Ti(1)–C(1)–C(3)/Ti(2)–C(5)–C(7) of 86.0(1)°, is similar to that of **3a** except the shorter tweezers arms. Ti(1)–Ag–Ti(2) is again linear with Ti–Ag distances of 3.267(3) and 3.248(3) Å. All four Ag–C(β) bonds (2.72(2)–2.81(2) Å) are longer

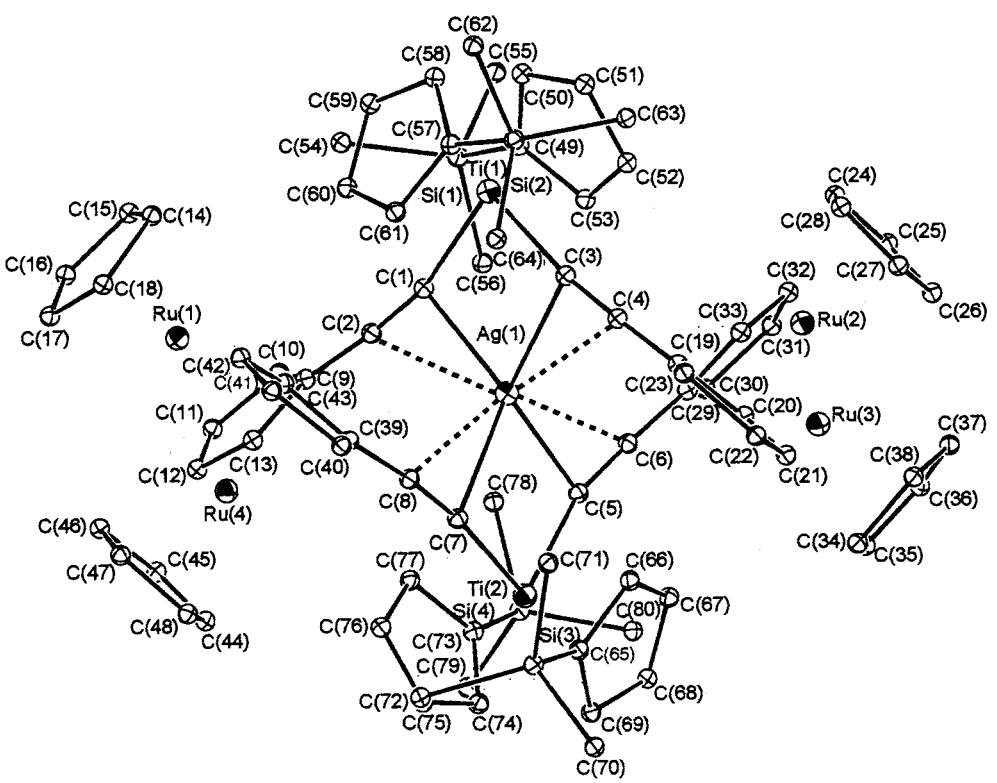

Fig. 2. Molecular structure of the cationic part of **4a** with the atomic numbering scheme.

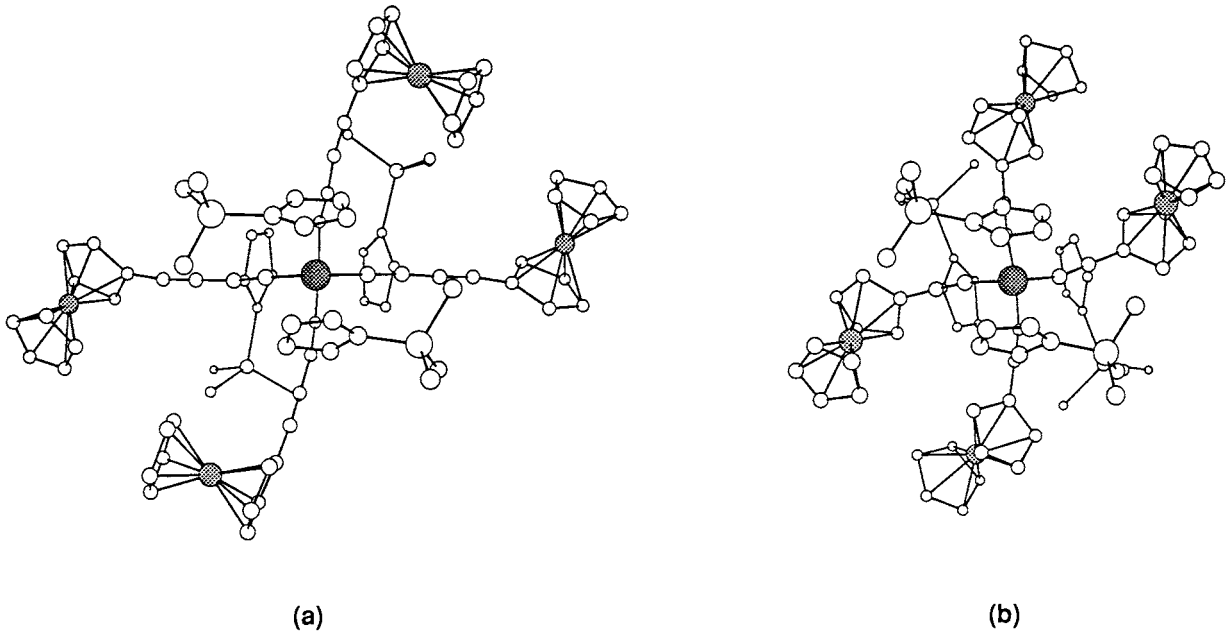

Fig. 3. View along the Ti–Ag–Ti axis. (a) Cationic part of **3a**; (b) cationic part of **4a**.

than in **6** by as much as 0.3–0.4 Å. This is brought about partly by longer Ti–Ag distances and partly by larger bend at C(1) and C(5) in **4a** (165(1) and 163(1)°) than the corresponding bend at C(α)'s of **6** (171(2) and 170(2)°).

When viewed along the axis Ti–Ag–Ti as shown in Fig. 3, it is apparent that the carbon rods are curved in a S-shaped way. This tendency is attributed to the steric repulsion between the large metallocenyl end groups at the rod-terminal with the cyclopentadienyl rings of titanocene of the aggregating partner. The shortest interatomic distance found in metallocenyl Cp carbon—titanocene Cp carbon is 3.22 Å in both **3a** and **4a**.

3. Experimental section

^{1}H- and ^{13}C-NMR spectra were measured on a JEOL JNM-EX270 spectrometer. IR spectra were recorded on a Perkin-Elmer 1600 FT-IR spectrometer. Mass spectra (FAB^+) were obtained on a J1EOL JMS-HX110 mass spectrometer. Mössbauer spectra were measured with a constant-acceleration type spectrometer, and the velocity scale was calibrated on the spectrum of metallic iron at room temperature. Spectra were fitted with Lorentzian line shapes by least squares. The isomer shifts were reported with respect to α-Fe foil at room temperature. The titanocene derivatives $(C_5H_4R)_2Ti\{(C{\equiv}C)_n\text{-}Mc\}_2$ (**1**–**4**) were prepared as reported previously [1] and $(C_5H_4SiMe_3)_2Ti(C{\equiv}CPh)_2$ (**5**) [16] were prepared by the literature method.

All manipulations were performed under argon. In addition, all reactions of $AgPF_6$ were carried out in a flask covered with aluminum foil to shield it from the light. Solvents were purified and distilled prior to use.

3.1. Synthesis of $[(C_5H_4R)_4Ti_2\{(C{\equiv}C)_n\text{-}Mc\}_4Ag](PF_6)$

3.1.1. $[(C_5H_5)_4Ti_2(C{\equiv}CC{\equiv}C{-}FC)_4Ag](PF_6)$ (**2a**)

To a CH_2Cl_2 solution (80 ml) of $(C_5H_5)_2Ti(C{\equiv}CC{\equiv}C{-}Fc)_2$ (**2**) (103 mg, 0.16 mmol) was added dropwise $AgPF_6$ (20 mg, 0.08 mmol) in CH_2Cl_2 (40 ml) at r.t. The reaction mixture was stirred for 30 min; it turned gradually from moss-green to light-green. After the solvent was evaporated, the residue was recrystallized from CH_2Cl_2/hexane at -30°C to give **2a** as deep green needles: yield 105 mg (85%). Anal. Calcd for $C_{76}H_{56}AgF_6Fe_4PSi_4Ti_2 \cdot 1/2CH_2Cl_2$: C, 58.02; H, 3.63; Ag, 7.00. Found: C, 57.83; H, 4.25; Ag, 6.81%. The presence of $1/2 \cdot CH_2Cl_2$ was also confirmed by ^{1}H-NMR measurement in acetone-d^6. ^{1}H-NMR (CD_2Cl_2) δ 6.51 (s, 20H, C_5H_5–Ti), 4.55 (bs, 8H, C_5H_4–Fe), 4.40 (bs, 8H, C_5H_4–Fe), 4.28 (s, 20H, C_5H_5–Fe). IR (CH_2Cl_2) ν(C≡C) 2161, 1988 cm^{-1}. MS (FAB^+) m/z 1395 $[M\text{-}(PF_6)]^+$.

Complexes **1a**, **3a** and **4a** were prepared in a similar manner.

3.1.2. $[(C_5H_4SiMe_3)_4Ti_2(C{\equiv}C{-}Fc)_4Ag](PF_6)$ (**1a**)

Yield 87%; blue-green needles. Anal. Calcd for $C_{80}H_{88}AgF_6Fe_4PSi_4Ti_2$: C, 55.42; H, 5.12; Ag, 6.22. Found: C, 55.21; H, 5.11; Ag, 6.30%. ^{1}H-NMR (CD_2Cl_2) δ 6.19 (t, $J = 2.3$ Hz, 8H, C_5H_4–Ti), 6.04 (t, $J = 2.3$ Hz, 8H, C_5H_4–Ti), 4.68 (t, $J = 1.8$ Hz, 8H,

C_5H_4–Fe), 4.57 (t, $J = 1.8$ Hz, 8H, C_5H_4–Fe), 4.34 (s, 20H, C_5H_5–Fe), 0.30 (s, 36H, TMS). IR (CH_2Cl_2) ν(C≡C) 2015 cm^{-1}. MS(FAB$^+$) m/z 1589 [M-(PF_6)]$^+$. Mössbauer parameters IS = 0.53, QS = 2.28 mm s^{-1}.

3.1.3. [($C_5H_4SiMe_3$)$_4$$Ti_2$(C≡CC≡C–Fc)$_4$Ag]($PF_6$) (**3a**)

Yield 92%; deep green needles. Anal. Calcd for $C_{88}H_{88}AgF_6Fe_4PSi_4Ti_2$: C, 57.76; H, 4.85; Ag, 5.89. Found: C, 57.71; H, 4.82; Ag, 5.71%. ^{1}H-NMR (CD_2Cl_2) δ 6.81 (t, $J = 2.3$ Hz, 8H, C_5H_4–Ti), 6.59 (t, $J = 2.3$ Hz, 8H, C_5H_4Ti), 4.54 (t, $J = 1.8$ Hz, 8H, C_5H_4–Fe), 4.40 (t, $J = 1.8$ Hz, 8H, C_5H_4–Fe), 4.26 (s, 20H, C_5H_5–Fe), 0.31 (s, 36H, TMS). IR (CH_2Cl_2) ν(C≡C) 2161, 1987 cm^{-1}. MS (FAB$^+$) m/z 1685 [M(PF_6)]$^+$. Mössbauer parameters IS = 0.53, QS = 2.28 mm s^{-1}.

3.1.4. [($C_5H_4SiMe_3$)$_4$$Ti_2$(C≡C–Rc)$_4$Ag]($PF_6$) (**4a**)

Yield 99%; red-purple crystals. Anal. Calcd for $C_{80}H_{88}AgF_6PRu_4Si_4Ti_2$: C, 50.18; H, 4.63; Ag, 5.63. Found: C, 49.94; H, 4.61; Ag, 5.57%. ^{1}H-NMR (CD_2Cl_2) δ 6.29 (t, $J = 2.3$ Hz, 8H, C_5H_4–Ti), 6.19 (t, $J = 2.3$ Hz, 8H, C_5H_4–Ti), 5.00 (t, $J = 1.6$ Hz, 8H, C_5H_4–Ru), 4.79 (t, $J = 1.6$ Hz, 8H, C_5H_4–Ru), 4.68 (s, 20H, C_5H_5–Ru), 0.26 (s, 36H, TMS). IR (CH_2Cl_2) ν(C≡C) 2020 cm^{-1}. MS (FAB$^+$) m/z 1770 [M-(PF_6)]$^+$.

Table 3
The crystal data of complexes **3a**·THF and **4a**

	3a·THF	**4a**
Formula	$C_{88}H_{88}AgFe_4Si_4Ti_2 \cdot PF_6 \cdot C_4H_8O$	$C_{80}H_{88}AgRu_4Si_4Ti_2 \cdot PF_6$
Molecular weight	1902.14	1914.84
Crystal size (mm)	0.35 × 0.20 × 0.07	1.40 × 1.00 × 0.25
Crystal system	Triclinic	Monoclinic
Space group	$P\bar{1}$	C_2/c
Unit cell dimensions		
a (Å)	16.692(8)	38.13(7)
b (Å)	17.105(3)	24.284(7)
c (Å)	18.054(2)	28.09(5)
α (°)	75.67(1)	90
β (°)	87.42(2)	105.36(2)
γ (°)	87.60(2)	90
V (Å^3)	4987	25080
Z	2	12
D_{calcd} (Mg m^{-3})	1.267	1.521
μ (mm^{-1})	10.163	15.739
Temperature (K)	298	298
Radiation	Mo–K_α (λ = 0.71073)	Mo–K_α (λ = 0.71073)
θ_{max} (°)	23.86	28.83
h, k, l ranges	−19 0, −20 20, −21 21	0 53, 0 34, −34 34
No. of reflections	18 322	24 853
No. of independent reflections	12 139	21 329
No. of reflections in ref. [$I \geq 3\sigma(I)$]	3461	12 969
No. of atoms and parameters	207, 480	186, 1326
Final R	0.094	0.076
Final Rw	0.116	0.092
Goodness of Fit	3.11	3.63
Max/min in diff. map (e Å^{-3})	1.91/−3.54	2.57/−1.67

3.2. Synthesis of [($C_5H_4SiMe_3$)$_4$$Ti_2$(C≡CPh)$_4$Ag]($PF_6$) (**5a**)

To a solution of ($C_5H_4SiMe_3$)$_2$Ti(C≡CPh)$_2$ (**5**) (84 mg, 0.16 mmol) in THF (80 ml) was added dropwise $AgPF_6$ (20 mg, 0.08 mmol) in THF (27 ml) at r.t. The reaction mixture was stirred for 30 min during which time the color turned gradually from orange to red-orange. After the solvent was evaporated, the residue was recrystallized from THF/hexane at −30°C to give **5a** as red-orange needles: yield 88 mg (85%). Anal. Calcd for $C_{64}H_{72}AgF_6PSi_4Ti_2$: C, 59.03; H, 5.57; Ag, 8.28. Found: C, 58.88; H, 5.69; Ag, 8.21%. ^{1}H-NMR (CD_2Cl_2) δ 7.70–7.49 (m, 20H, Ph), 6.24 (t, $J = 2.3$ Hz, 8H, C_5H_4–Ti), 6.03 (t, $J = 2.3$ Hz, 8H, C_5H_4–Ti), 0.08 (s, 36H, Me). IR (THF) ν(C≡C) 2039 cm^{-1}. MS (FAB$^+$) m/z 1157 [M-(PF_6)]$^+$.

3.3. X-ray crystal analysis

A deep green crystal of **3a** grown in THF at 5°C was mounted in a glass capillary with a small volume of mother liquor. The X-ray measurements were performed on a Mac Science MXC18 diffractometer with graphite-monochromated Mo–K_α radiation ($\lambda = 0.7107$ Å) at r.t. in the dark.

Deep purple crystals of **4a** were grown in CH_2Cl_2/hexane at r.t. Oscillation and nonscreen Weissenberg photographs were recorded on the imaging plates on Mac Science DIP3000 with an 18-kW rotating anode generator. Data reduction and determination of cell parameters were made by MAC DENZO program system.

The structures were solved by direct methods using SIR92 in the CRYSTAN-GM program system (software package for structure determination) and refined by full-matrix least-squares procedures. Hydrogen atoms were not located. The crystallographic and refinement parameters are summarized in Table 3.

References

[1] Y. Hayashi, M. Osawa, Y. Wakatsuki, J. Organomet. Chem. 542 (1997) 241.
[2] Y. Hayashi, M. Osawa, K. Kobayashi, Y. Wakatsuki, Chem. Commun. (1996) 1617.
[3] S. Back, H. Pritzkow, H. Lang, Organometallics 17 (1998) 41.

[4] J.R. Berenguer, L.R. Falvello, J. Fornies, E. Lalinde, M. Tomas, Organometallics 12 (1993) 6.
[5] M.D. Janssen, M. Herres, L. Zsolnai, D.M. Grove, A.L. Spek, H. Lang, G.V. Koten, Organometallics 14 (1995) 1098.
[6] M.D. Janssen, M. Herres, A.L. Spek, D.M. Grove, H. Lang, G.V. Koten, J. Chem. Soc. Chem. Commun. (1995) 925.
[7] H. Lang, L. Zsolnai, J. Organomet. Chem. 406 (1991) 5.
[8] H. Lang, M. Herres, L. Zsolnai, W. Imhof, J. Organomet. Chem. 409 (1991) 7.
[9] H. Lang, W. Imhof, Chem. Ber. 125 (1992) 1307.
[10] H. Lang, M. Herres, L. Zsolnai, Organometallics 12 (1993) 5008.
[11] H. Lang, K. Kohler, B. Schiemenz, J. Organomet. Chem. 495 (1995) 135.
[12] H. Lang, K. Kohler, L. Zsolnai, Chem. Commun. (1996) 2043.
[13] S. Yamazaki, A. J. Deeming, J. Chem. Soc. Dalton Trans. (1993) 3051.
[14] I. Ara, J.R. Berenguer, J. Fornies, E. Lalinde, M.T. Moreno, J. Organomet. Chem. 510 (1996) 63.
[15] M.G. Hill, W.M. Lamanna, K.R. Mann, Inorg. Chem. 30 (1991) 4687.
[16] J.H. Teuben, H.J.D. L. Meijer, J. Organomet. Chem. 17 (1969) 87.